Eur. J. Biochem. **265**, 627–637 (1999) © FEBS 1999

Host defence peptides from the skin glands of the Australian Blue Mountains tree-frog *Litoria citropa*

Solution structure of the antibacterial peptide citropin 1.1

Kate L. Wegener[1], Paul A. Wabnitz[1], John A. Carver[2], John H. Bowie[1], Brian C. S. Chia[1], John C. Wallace[3] and Michael J. Tyler[4]

[1]*Department of Chemistry, The University of Adelaide, South Australia, Australia;* [2]*Department of Chemistry, University of Wollongong, New South Wales, Australia;* [3]*Department of Biochemistry, The University of Adelaide, South Australia, Australia;* [4]*Department of Environmental Biology, The University of Adelaide, South Australia, Australia*

Nineteen citropin peptides are present in the secretion from the granular dorsal glands of the Blue Mountains tree-frog *Litoria citropa*; 15 of these peptides are also present in the secretion from the submental gland. Two major peptides, citropin 1.1 (GLFDVIKKVASVIGGL-NH_2), citropin 1.2 (GLFDIIKKVASVVGGL-NH_2) and a minor peptide, citropin 1.3 (GLFDIIKKVASVIGGL-NH_2) are wide-spectrum antibacterial peptides. The amphibian has an endoprotease which deactivates these membrane-active peptides by removing residues from the N-terminal end: loss of three residues gives the most abundant degradation products. The solution structure of the basic peptide citropin 1.1 has been determined by NMR spectroscopy [in a solvent mixture of trifluoroethanol/water (1 : 1)] to be an amphipathic α-helix with well-defined hydrophobic and hydrophilic regions. The additional four peptides produced by the dorsal glands are structurally related to the antibacterial citropin 1 peptides but contain three more residues at their C-terminus [e.g. citropin 1.1.3 (GLFDVIKKVASVIGLASP-OH)]. These peptides show minimal antibacterial activity; their role in the amphibian skin is not known.

Keywords: antibacterial peptides; sequencing; NMR; solution structure; amphipathic helix.

Amphibians have rich chemical arsenals in the skin glands that form an integral part of their defence system, and also assist with the regulation of dermal physiological action [1,2]. In response to a variety of stimuli, host defence compounds are secreted from these specialized glands onto the dorsal surface and into the gut of the amphibian. Some of these compounds are antibacterial peptides, e.g. the bombinin, brevinin and magainin families of peptides [2–4]. The magainin peptides also show some anti-cancer activity [5]. Some of the antibacterial peptides have attracted pharmaceutical interest [6].

The dermal secretions of some Australian tree-frogs (*Litoria splendida*, *L. caerulea*, *L. gilleni*, *L. xanthomera*, *L. chloris* and *L. genimacula*) collectively contain more than 30 antibacterial peptides [7–14]. The major wide-spectrum antibacterial agents from these tree-frogs belong to either the caerin or maculatin families of peptides. Particular examples are caerin 1.1 (one of 10 structurally related peptides from *L. splendida*, *L. caerulea*, *L. gilleni*, *L. chloris* and *L. xanthomera*) and maculatin 1.1 (from *L. genimaculata*). These peptides are, respectively, 25 and 21 amino acids in length: their sequences are related but maculatin 1.1 is missing four amino acid residues from the centre of a caerin 1-type sequence. The two peptides have the following sequences:

Caerin 1.1 GLLSVLGSVAKHVLPHVVPVIAEHL-NH_2
Maculatin 1.1 GLFGVLAKVAAHVVPAIAEHF-NH_2

The solution structures of both peptides have been investigated by NMR spectroscopy. In trifluoroethanol/water mixtures, caerin 1.1 adopts two well-defined helices (Leu2 to Lys11 and from Val17 to His24) separated by a hinge region of less-defined helicity and greater flexibility [15]. In contrast to caerin 1.1, maculatin 1.1 does not have such marked flexibility in its central region. In this case, NMR spectra [measured (a) in trifluoroethanol/water and (b) with the peptide incorporated into an artificial phospholipid micelle] show that the amphipathic α-helix of maculatin 1.1 is distorted by Pro15: the central axis of the helix preceding Pro15 makes an angle of approximately 20° to the axis of the helix following Pro15 [16].

Amphipathic peptides of this type are membrane-active antibacterial agents. Interaction occurs at the membrane surface with the charged (normally basic) peptide adopting an α-helical conformation and attaching itself to charged sites (normally anionic) on the lipid bilayer. Two potential mechanisms have been proposed for interaction of these peptides with membranes, viz: aggregation of peptides is followed either by (a) penetration through the lipid bilayer via formation of a transmembrane helical bundle (the barrel-stave mechanism) or (b) formation of pores through the membrane as a result of the alignment of the peptides parallel to the membrane surface (the 'carpet' mechanism). As a result, disruption of normal membrane function occurs leading to lysis of the cell [17–22]. The magainin peptides (from the African clawed frog *Xenopus laevis*) are the best studied of such amphibian peptides. NMR

Correspondence to J. H. Bowie, Department of Chemistry, The University of Adelaide, South Australia, 5005, Australia, Fax: + 61 88303 4358, Tel.: + 61 88303 5767, E-mail: jbowie@chemistry.adelaide.edu.au

Abbreviations: ALLHDG, all hydrogen distance geometry; DQF COSY, double-quantum-filtered correlation spectroscopy; ESMS, electrospray mass spectroscopy; HMBC, heteronuclear multiple-bond correlation; HSQC, heteronuclear single-quantum coherence; MIC, minimum inhibitory concentration; NOESY, nuclear Overhauser effect spectroscopy; RMD, restrained molecular dynamics; SA, simulated annealing; TOCSY, total correlation spectroscopy; TFE, trifluoroethanol.

(Received 25 May 1999, revised 22 July 1999, accepted 23 July 1999)

studies show they form well-defined amphipathic α-helices in solution and when incorporated into an artificial phospholipid; the peptides are positively charged and interact readily with anionic phospholipids [6,18,21–23]. As caerin 1.1 and maculatin 1.1 are also membrane-active basic peptides, then perhaps they react in a similar manner to the magainins. Although the solution structures of caerin 1.1 and maculatin 1.1 are quite different, the antibacterial activities of each peptide are very similar [15,16]. If they are synthetically modified to convert them into molecules with better defined α-helical structures, i.e. removal of the hinge of caerin 1.1 by conversion of both Pro residues to Ala, or distortion of maculatin 1.1 by conversion of Pro15 to Ala15, the spectrum of antibacterial activities is significantly reduced in each case.

In this paper we describe the isolation, sequence determination, and activities of the citropin peptides from the Blue Mountain tree-frog of Australia, *L. citropa*. This frog is found near flowing, rocky streams in heavily forested areas from the coast to the Dividing Ranges in eastern Victoria and New South Wales. The length of the adult frog is in the range 4.5–5.6 cm, and the frog can be distinguished by its brown dorsum, green flash colours near the head, and by a brown tympanum [24,25]. This tree-frog is unusual in that it has two types of skin glands, the granular glands on the dorsal surface and the large submental gland on the throat. Other Australian tree-frogs that we have studied have no submental gland, thus it is of interest to determine the role of this gland, for example, does it contain host defence peptides like the dorsal glands of other amphibians, and if so, whether these peptides are similar in activity and structure to the caerin 1 and maculatin 1 peptides.

EXPERIMENTAL PROCEDURES

Preparation of skin secretions

L. citropa was held by the back legs, the skin moistened with deionized water, and the two types of glands (i.e. the granular dorsal glands situated on the back, and the submental gland situated on the throat) were stimulated independently by means of a bipolar electrode of 21G platinum attached to a Palmer Student Model electrical stimulator. The electrode was rubbed gently in a circular manner on the particular gland (under study) of the animal, using 10 V and a pulse duration of 3 ms [26]. The resulting secretion was washed from the frog with deionized water (50 mL), the mixture diluted with an equal volume of methanol, centrifuged, filtered through a Millex HV filter unit (0.45 μm), and lyophilized. This procedure provided, on average, some 5 mg of solid material from the dorsal glands and 3 mg from the submental gland. This work conforms with the Code of Practice for the Care and Use of Animals for Scientific Purposes (1990) and the Prevention of Cruelty to Animals Act 1985, and was approved by the University of Adelaide Animal Ethics Committee.

HPLC Separation of the glandular secretion

HPLC separation was achieved using a VYDAC C18 HPLC column (5 μ, 300 A, 4.6 × 250 mm) (Separations Group, Hesperia, CA, USA) equilibrated with 10% acetonitrile/aqueous 0.1% trifluoroacetic acid. The lyophilized mixture (generally ≈ 1 mg) (see above) was dissolved in deionized water (50 μL), of which a 10-μL fraction was injected into the column. The elution profile was generated using a linear gradient produced by an ICI DP 800 Data Station controlling two LC1100 HPLC pumps, increasing from 10 to 75% acetonitrile

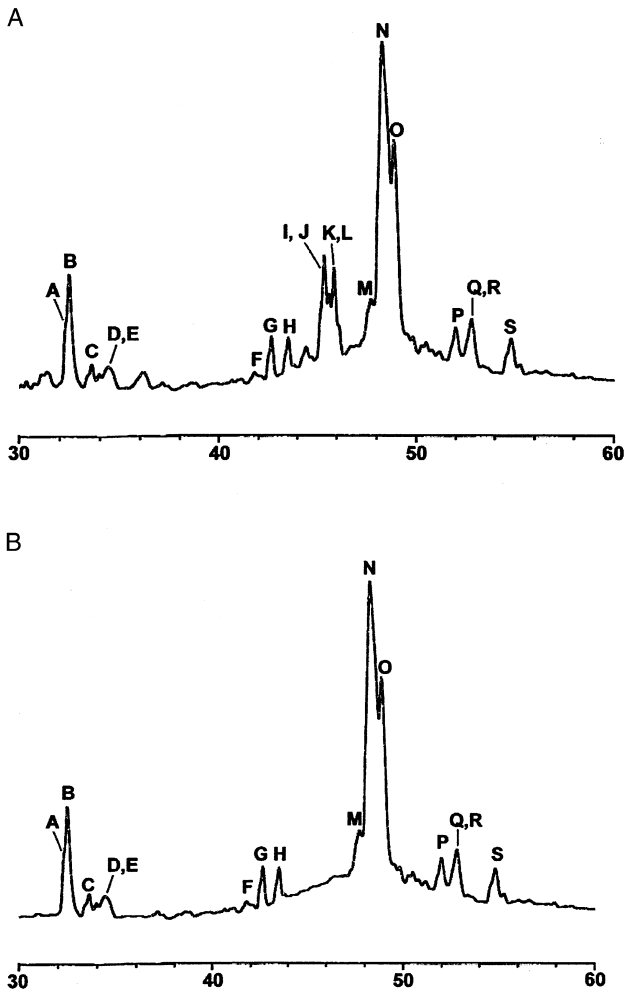

Fig. 1. HPLC separations of the citropin peptides secreted by the dorsal glands (A) and the submental gland (B) of *Litoria citropa*. Fractions are labelled A to S, the amino acid sequences of the peptides from each fraction are listed in Table 1. Components were obtained pure by further HPLC separation except for those in the two fractions D/E and Q/R which could not be resolved even after repeated HPLC experiments.

over a period of 60 min at a flow rate of 1 mL·min^{-1}. The eluant was monitored by ultraviolet absorbance at 214 nm using an ICI LC-1200 variable wavelength detector (ICI Australia, Melbourne, Australia). The HPLC traces of the antibacterial peptide regions of each glandular extract (Fig. 1) are complex: 17 fractions were investigated. Fractions were collected, concentrated and dried *in vacuo* for subsequent analysis. Further HPLC separation was required for some fractions in order to obtain pure components.

Sequence determination of peptides

Electrospray mass spectroscopy. Electrospray mass spectra were determined using a Finnigan LCQ ion trap mass spectrometer. Purified fractions from the HPLC separation were dissolved in methanol/water (1 : 1, v/v) and infused into the electrospray source at 8 μL·min^{-1}. Electrospray conditions were as follows: needle potential 4.5 kV, tube lens 60 V, heated capillary 200 °C and 30 V, sheath gas flow 208 kPa. Mass spectra were acquired with the automatic gain control on, a maximum time of 400 ms, and averaging over three microscans. Molecular masses of peptides less than 2000 Da in mass

were determined from $(M + H)^+$ ions; those greater than 2000 Da in mass were determined from $(M + 2H)^{2+}$ ions. All peptides were methylated to form methyl esters. The mass of the MH^+ parent ion of the methyl ester minus that of the MH^+ of the original peptide allows the determination of the number of CO_2H and $CONH_2$ groups in the molecule (viz CO_2H gr; CO_2Me = 14 Da, whereas $CONH_2$ gr; CO_2Me = 15 Da) [8].

Protein sequencing. Automated Edman sequencing was performed by a standard procedure [27] using an applied Biosystem 492 procise sequencer equipped with a 900-A data analysis module. The best results were obtained using a disc of immobilon film treated with bioprene in ethanol, onto which the peptide was absorbed from aqueous acetonitrile (90%). The disc was pierced several times with a razor blade to aid the flow of solvent.

Preparation of synthetic peptides

Ten natural citropin peptides and two modified citropin 1.1 peptides were synthesized (by Chiron Mimotopes, Clayton, Victoria, Australia) using L-amino acids via the standard *N*-α-Fmoc method (full details including protecting groups and deprotection have been reported recently [28]). Each synthetic citropin was shown to be identical with the natural citropin by both electrospray MS and HPLC. The sample of citropin 1.1 prepared for the NMR study was 91% pure (by HPLC and electrospray MS).

Antimicrobial testing

Antimicrobial testing on synthetic citropin peptides was carried out by the Microbiology Department of the Institute of Medical and Veterinary Science (Adelaide, Australia). The method used involved the measurement of inhibition zones (produced by the applied peptide) on a thin agarose plate containing the microorganisms under study. The procedures are standard [29]. Activities are recorded as the minimum inhibitory concentration (MIC) of peptide per mL required to totally inhibit the growth of the named microorganism.

CD spectroscopy

CD spectra were recorded on a Jobin-Yvon CD-6 spectrophotometer at room temperature. CD spectra of citropin 1.1, at a concentration of 31 μM, were acquired in solutions of TFE in water (0–50% by volume). Each spectrum represents the average of five scans, with the data smoothed over $n = \pm 5$ data points.

NMR spectroscopy of citropin 1.1

NMR experiments were carried out on a solution of 8 mg of citropin 1.1 dissolved in a mixture of water (0.35 mL) and d_3-TFE (0.35 mL), giving a final concentration of 7.1 mM, at a measured pH of 2.25.

NMR spectra were acquired on a Varian Inova-600 NMR spectrometer, at a ^1H frequency of 600 MHz and ^{13}C frequency of 150 MHz. All NMR experiments were performed at 25 °C. ^1H NMR spectra were referenced to the methylene protons of residual TFE (3.918 p.p.m.). The ^{13}C (F_1) dimensions of the heteronuclear single-quantum coherence (HSQC) and heteronuclear multiple-bond correlation (HMBC) spectra were referenced to the $^{13}CH_2$ (60.975 p.p.m.) and $^{13}CF_3$ (125.9 p.p.m.) resonances of TFE, respectively.

Double-quantum-filtered correlation spectroscopy (DQF-COSY) [30]; total correlation spectroscopy (TOCSY) [31]; and nuclear Overhauser effect spectroscopy (NOESY) [32]; were all collected in the phase-sensitive mode using time proportional phase incrementation [33] in t_1. For each of these experiments, 256 t_1 increments were used. In the TOCSY and DQF-COSY experiments, 16 scans were time averaged for each increment, while 48 scans were averaged in the NOESY experiments. The free induction decay in t_2 consisted of 2048 data points over a spectral width of 5564.1 Hz. The transmitter frequency was centred on the water resonance; conventional low power presaturation from the same frequency synthesizer was applied during a 1.5-s relaxation delay to suppress the large water signal in the TOCSY and NOESY spectra. Gradient methods for water suppression were used in the DQF-COSY spectrum [34]. The TOCSY spectrum was acquired with the pulse sequence used by Griesinger *et al*. [35], which minimizes cross relaxation effects by employing an MLEV-17 spin-lock of 70 ms duration. NOESY spectra were acquired with mixing times of 80, 150 and 250 ms.

An HSQC experiment [36] was acquired to assign the α-^{13}C resonances via correlations to their attached protons. The interpulse delay was set to $1/2J_{CH}$ = 3.6 ms corresponding to J_{CH} = 140 Hz. For this experiment, 256 t_1 increments, each comprising 16 time averaged scans, were acquired over 2048 data points and 5564.1 Hz in the directly detected (^1H, F_2) dimension. In the ^{13}C (F_1) dimension a spectral width of 24 140 Hz was used. An HMBC spectrum [37] was collected to assign the carbonyl-^{13}C resonances via correlations through two and three bonds to α, β and NH protons (with an interpulse delay, $1/2J_{CH}$ = 62.5 ms for J_{CH} = 7 Hz). In this experiment 512 t_1 increments, each comprising 64 scans, were acquired over 4096 data points and 5564.1 Hz in the ^1H (F_2) dimension. The spectral width for the ^{13}C (F_1) dimension was 40 000 Hz.

All 2D NMR spectra were processed on a Sun Microsystems Ultra Sparc 1/170 workstation using VNMR software (v 6.1a). The data matrices were multiplied by a Gaussian function in both dimensions and then zero-filled to 2048 data points in F_1 prior to Fourier transformation, except in the case of the HMBC experiment where zero-filling was carried out on 4096 data points in F_1. Final processed 2D NMR matrices consisted of 2048 × 2048 or 4096 × 4096 real points.

Structural constraints

Cross-peaks in the TOCSY and NOESY (mixing time = 150 ms) spectra were assigned using XEASY software (v 1.3.13) [38]. The volumes for these cross-peaks were converted to distance constraints using the method of Xu *et al*. [39]. For each symmetrical pair of cross-peaks, the peak of smaller volume was used. This procedure generated 230 distance constraints. Of these, 133 were intraresidue constraints, 50 were sequential (i, $i + 1$) constraints and 47 were medium range constraints (from two to four residues distant). Twenty-six of the distance constraints were ambiguous.

$^3J_{NHC\alpha H}$ values were measured from a high-resolution 1D ^1H NMR spectrum acquired with 0.012 Hz per point digital resolution (128 000 data points). Dihedral angles were restrained as follows: $^3J_{NHC\alpha H} < 5$ Hz, $\phi = -60° \pm 30°$; $5 < {}^3J_{NHC\alpha H} < 6$ Hz, $\phi = -60° \pm 40°$. Where $^3J_{NHC\alpha H} > 6$ Hz, φ angles were not constrained. The absence of resolved splitting for an NH resonance implies that its $^3J_{NHC\alpha H}$ value is < 5 Hz, i.e. the particular amino acid is part of a helical conformation. Hence, the φ angles for these types of residues

Table 1. The amino acid sequences of the citropin peptides from *Litoria citropa*. The nominal mass, equal to the sum of the integral masses of the amino acids, is shown. The designation of fractions in HPLC separation traces are shown in Figs 3 and 4. D, dorsal (on the back); S, submental (on the throat).

Citropin	Sequence	Mass	HPLC fraction	Gland
1.1	GLFDVIKKVASVI GGL-NH_2	1614	N	D, S
1.1.1	FDVIKKVASVI GGL-NH_2	1444	E	D, S
1.1.2	DVIKKVASVI GGL-NH_2	1297	B	D, S
1.1.3	GLFDVIKKVASVI GLASP-OH	1813	J	D
1.1.4	GLFDVIKKVASVI GLASQ-OH	1844	L	D
1.2	GLFDIIKKVASVVGGL-NH_2	1614	O	D, S
1.2.1	FDIIKKVASVVGGL-NH_2	1444	D	D, S
1.2.2	DIIKKVASVVGGL-NH_2	1297	A	D, S
1.2.3	GLFDIIKKVAS-NH_2	1189	C	D, S
1.2.4	GLFDIIKKVASVVGLASP-OH	1813	K	D
1.2.5	GLFDIIKKVASVVGLASQ-OH	1844	I	D
1.3	GLFDIIKKVASVI GGL-NH_2	1628	M	D, S
2.1	GLIGSIGKALGGLLVDVLKPKL-OH	2160	S	D, S
2.1.1	GLIGSIGKALGGLLVDVLKPKLQ-OH	2288	Q	D, S
2.1.2	GLIGSIGKALGGLLVDVLKPKLQAA-OH	2430	R	D, S
2.1.3	GLIGSIGKALGGLLVDVLKPKLQAAS -OH	2517	P	D, S
3.1	DLFQVIKEKLKELTGGVIEGIQ-OH	2513	F	D, S
3.1.1	DLFQVIKEKLKELTGGVIEGIQG-OH	2546	G	D, S
3.1.2	DLFQVIKEKLKELTGGVIEGIQGV-OH	2612	H	D, S

Table 2. Antibacterial activities of some natural and modified citropin peptides from litoria citropa. Comparison with the antibacterial activities of caerin 1.1, maculatin 1.1 and uperin 3.6. MIC, minimum concentration of the peptide in $\mu g \cdot mL^{-1}$ necessary to inhibit the growth of the pathogen; sm, syn mod.

Peptide	Sequence	MIC >100 $\mu g \cdot mL^{-1}$
Citropin		
1.1	GLFDVIKKVASVIGGL-NH_2	
1.1 sm 1	GLFAVIKKVASVIGGL-NH_2	
1.1 sm 2	GLFDVIAKVASVIGGL-NH_2	
1.1.2	DVIKKVASVIGGL-NH_2	Yes
1.1.3	GLFDVIKKVASVIGLASP-NH_2	
1.2	GLFDIIKKVASVVGGL-NH_2	
1.2.2	DIIKKVASVVGGL-NH_2	Yes
1.2.3	GLFDIIKKVAS-NH_2	Yes
1.3	GLFDIIKKVASVIGGL-NH_2	
2.1	GLIGSIGKALGGLLVDVLKPKL-OH	
2.1.3	GLIGSIGKALGGLLVDVLKPKLQAAS-OH	
3.1.2	DLFQVIKEKLKELTGGVIEGIQGV-OH	Yes
Caerin 1.1	GLLSVLGSVAKHVLPHVVPVIAEHL-NH_2	
Maculatin 1.1	GLFGVLAKVAAHVVPAIAEHF-NH_2	
Uperin 3.6	GVIDAAKKVVNVLKNLF-NH_2	

	MIC ($\mu g \cdot mL^{-1}$)[a]										
Bacterium	1.1	sm1	sm2	1.1.3	1.2	1.3	2.1	2.1.3	C1.1	M1.1	U3.6
Bacillus cereus	50	25	100		25	25			50	25	25
Escherichia coli		100									
Leuconostoc lactis	6	3	25	50	3	6	50	100	1.5	3	3
Listeria innocua	25	25			100	25			25	100	50
Micrococcus luteus	12	12	100		12	12			12	12	50
Pasteurella multocida										25	50
Staphylococcus aureus	25	25	100		25	25			3	6	25
Staphylococcus epidermidis	12	12	100		25	25			12	12	12
Streptococcus uberis	25	25	100	100	12	12			12	3	12

[a] If there is no figure listed the MIC value is > 100 $\mu g \cdot mL^{-1}$.

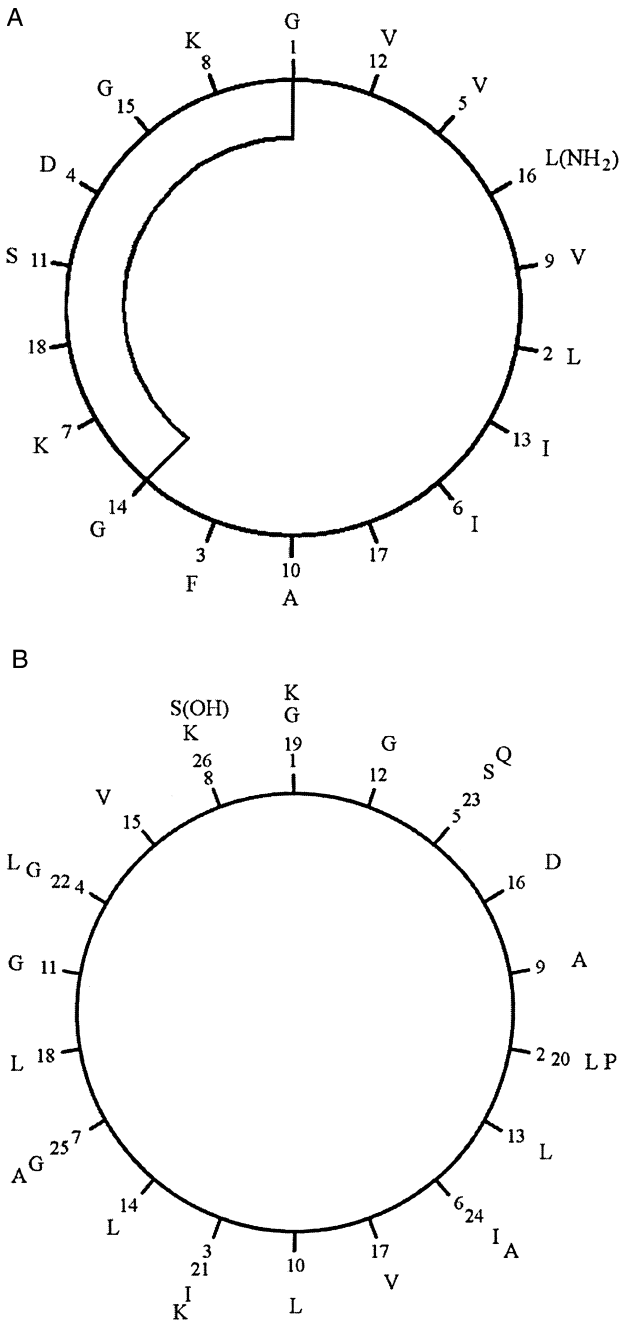

Fig. 2. The Edmundson projection of citropins 1.1. (A) and 2.1.3 (B). Note the well-defined hydrophobic and hydrophilic regions represented by the right and left-hand sides of the figure, respectively.

were restrained to $-60° \pm 30°$. A total of five dihedral angle restraints were used for the structure calculations.

Structural calculations

Structures were generated on a Sun Microsystems Sparc 1/170 workstation using XPLOR software (v 3.851) [40,41]. The restrained molecular dynamics (RMD) and dynamical simulated annealing (SA) protocol was used [42], including the use of floating stereospecific assignments [43]. Sum-averaging was employed to account for the ambiguous constraints. The ALL HYDROGEN DISTANCE GEOMETRY (ALLHDG) force field (v 4.03) was employed for all calculations [44]. Initially a family of

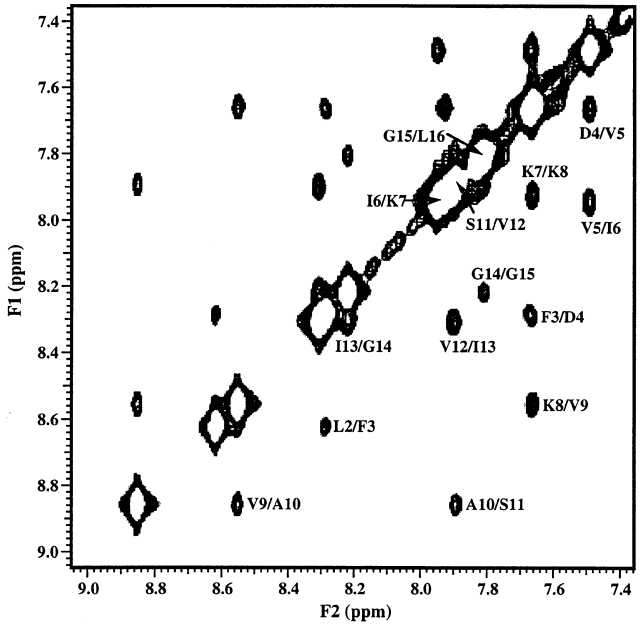

Fig. 3. NH to NH region of a NOESY spectrum (mixing time = 150 ms) of citropin 1.1 in 50% (v/v) d_3-TFE. NOEs between sequential NH protons are indicated.

60 structures was generated with random ϕ and ψ dihedral angles. These were subjected to 6500 steps (19.5 ps) of high temperature dynamics at 2000 K. The Knoe and Krepel force constants were increased from 1000 to 5000 kcal·mol^{-1}·nm^{-2} and 200–1000 kcal·mol^{-1}·nm^{-4}, respectively. This was followed by 2500 steps (7.5 ps) of cooling to 1000 K with Krepel increasing from 1000 to 40000 kcal·mol^{-1}·nm^{-4} and the atomic radii decreased from 0.9 to 0.75 times those in the ALLHDG parameter set. The last step involved 1000 steps (3 ps) of cooling from 1000 K to 100 K. Final structures were subjected to 200 steps of conjugate gradient energy minimization. The 20 structures produced with the lowest potential energies were selected for analysis. 3D structures were displayed using INSIGHT II software (v 95.0, MSI).

RESULTS

Isolation, sequence determination and antibacterial activity of the citropin peptides.

A single specimen of *L. citropa* was kept in captivity for several years and an electrical stimulation procedure [26] was used to obtain glandular secretions. This can be carried out on a monthly basis without harming the animal. Mild electrical stimulation of the skin in the vicinity of (a) the granular dorsal glands, and (b) the submental gland, gave two glandular secretions: each of these was subjected to HPLC separation; those regions of the HPLC traces containing the antibacterial peptides are shown in Fig. 1. Nineteen peptides were identified and characterized following HPLC separation. The amino acid sequences of the 19 characterized peptides are listed in Table 1. We have named these peptides citropins. Fifteen of the citropin peptides are produced by both the dorsal and submental glands, however, there are four additional peptides produced only by the dorsal glands.

There are three groups of citropins, designated citropins 1–3, respectively. Eight of the peptides of the citropin 1 group are

Table 3. ^{1}H and ^{13}C NMR chemical shifts for citropin 1.1 in TFE/H_2O (1 : 1, v/v), at a measured pH of 2.25 at 25 °C. Assignments for all the ^{1}H NMR resonances are presented whereas only the α-^{13}C and carbonyl-^{13}C resonances are tabulated; NO, not observed.

	Chemical shift (p.p.m.)					
Residue	NH	α-CH	β-CH	Others	α^{13}CH	^{13}CO
Gly1	NO	4.03, 3.90			44.9	170.5
Leu2	8.61	4.13	1.57	γ-CH 1.57 δ-CH_3 0.92, 0.86	57.0	177.2
Phe3	8.28	4.35	3.13	H2,6 7.34 H3,5 7.23 H4 7.29	59.4	177.6
Asp4	7.66	4.38	2.94		55.6	176.9
Val5	7.48	3.68	2.33	γ-CH_3 1.04, 0.95	65.3	176.7
Ile6	7.94	3.64	1.86	γ-CH_2 1.67, 1.22 γ-CH_3 0.91 δ-CH_3 0.83	64.0	176.9
Lys7	7.91	3.91	1.77	γ-CH_2 1.47, 1.35 δ-CH_2 1.66 ε-CH_2 2.90 ε-NH_3^+ 7.57	58.6	178.5
Lys8	7.66	4.13	2.14, 2.03	γ-CH_2 1.59, 1.32 δ-CH_2 1.75, 1.67 ε-CH_2 2.94, 2.86 ε-NH_3^+ 7.60	58.0	178.3
Val9	8.55	3.60	2.18	γ-CH_3 1.05, 0.95	66.0	177.5
Ala10	8.84	4.04	1.48		54.2	179.9
Ser11	7.88	4.29	4.13, 4.06		60.3	175.0
Val12	7.89	3.94	2.30	γ-CH_3 1.07, 0.97	64.5	177.7
Ile13	8.30	3.97	1.97	γ-CH_2 1.59, 1.32 γ-CH_3 0.94 δ-CH_3 0.83	62.8	177.6
Gly14	8.22	3.99, 3.90			42.3	174.6
Gly15	7.80	4.08, 3.93			44.4	173.8
Leu16	7.82	4.33	1.79	γ-CH 1.61 δ-CH_3 0.93, 0.88 $CONH_2$ 7.29, 6.77	54.3	179.6

post-translationally modified, in that they have C-terminal $CONH_2$ functionality. In contrast, four citropins 1 and all of the citropins 2 and 3 have C-terminal CO_2H groups. Citropins 1.1, 1.2 and 1.3 can be represented by Edmundson projections in which the α-helical conformations have well-defined hydrophilic and hydrophobic zones (see, e.g. Fig. 2A for citropin 1.1). This suggests the possibility that citropins 1.1, 1.2 and 1.3 may be amphipathic α-helical peptides exhibiting antibacterial activity.

The situation concerning the citropins 2 and 3 is not as straightforward, however. Both groups of peptides have C-terminal CO_2H groups, a function which generally results in reduction in antibacterial activity of amphibian peptides [1,2,45,46]. The Edmundson projections of the citropins 2 and 3 do not show such well-defined hydrophilic and hydrophobic zones as do those of the citropins 1 (see Fig. 2B for citropin 2.1.3). However, such peptides will not be able to form ideal α-helices because the presence of central Gly and/or Pro residues have a destabilizing influence on helical formation [15]. For example, citropin 2.1.3 contains Gly4, 7, 11 and 12 together with Pro20. Therefore, it is difficult to predict whether citropins 2 and 3 will show antibacterial or other bio-activity.

The 10 natural citropins shown in Table 2 were synthesized, their antimicrobial activities determined against the bacteria listed in Table 2, and the corresponding activities of caerin 1.1 and maculatin 1.1 (and uperin 3.6, see later) are included for comparison. Citropins 1.1, 1.2 and 1.3 show antibacterial activity against the same pathogens affected by caerin 1.1 and maculatin 1.1 (except that they show no activity against *Pasteurella multocida*, see Table 2). The wide-spectrum antibacterial activity of the three citropins 1 is more pronounced against Gram-positive than Gram-negative organisms. Neither citropin 2 nor citropin 3 peptides show significant activity against bacteria (Table 2).

Two synthetic modifications of citropin 1.1 (Ala4 and Ala7 citropin 1.1) were prepared in order to determine the importance of the hydrophilic Asp and Lys residues on the antibacterial activity of citropin 1.1. These data are also listed in Table 2. The residue Asp4 is not essential for antibacterial activity: indeed, replacement of Asp4 with Ala4 marginally

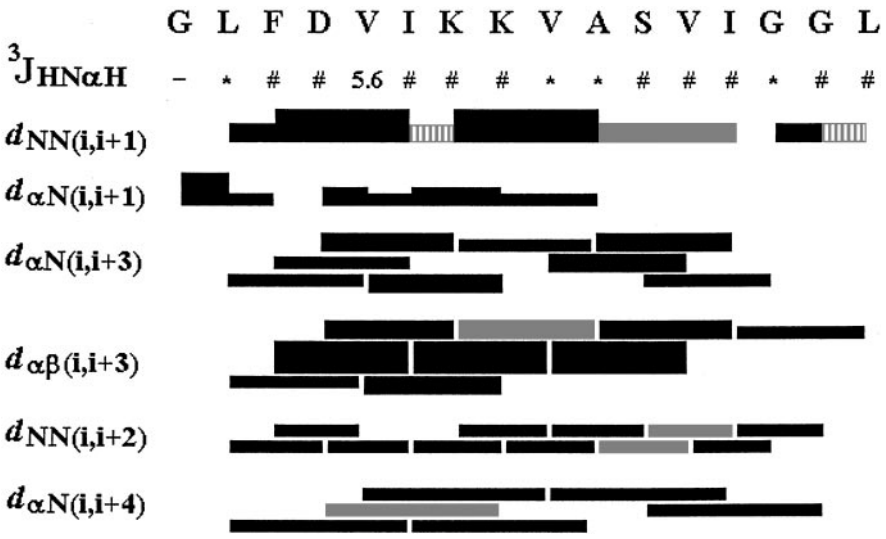

Fig. 4. Summary of NOEs used for structure calculation of citropin 1.1 in 50% (v/v) d_3-TFE. The thickness of the bars indicates the relative strength of the NOEs as indicated by the restraints generated from them, i.e. strong (0.18–0.31 nm), medium (0.18–0.37 nm) and weak (0.18–0.50 nm). Grey shaded boxes represent NOEs that could not be unambiguously assigned due to overlap, e.g. with an intraresidue NOE. Striped boxes indicate cross-peaks would be too close to the diagonal to be identified if present. The $^3J_{NHC\alpha H}$ values, where possible as determined from high-resolution 1D ^{1}H NMR spectra, are indicated. An asterisk (*) indicates the *J* coupling was not resolved while a cross-hatch (#) indicates the coupling constant could not be reliably determined due to overlap.

increases the antibacterial activity. In contrast, replacement of Lys7 with Ala7 significantly reduces the antibacterial activity of the peptide.

The solution structure of citropin 1.1

The interesting features of citropins 1.1, 1.2 and 1.3 are that they are very simple basic peptides that, with only 16 amino acid residues, are not long enough (when in an α-helical conformation) to traverse the lipid bilayer of a bacterial cell (e.g. via the 'barrel stave' mechanism: a minimum of 20 residues is needed for such a mechanism [19–21]). A prerequisite for antibacterial membrane activity may involve some aggregation of citropin 1 molecules on the membrane surface before the bacterial cell wall can be breached, e.g. via the so called 'carpet' mechanisms for the disruption of membrane function [19,20]. Do the citropins 1 adopt well-defined α-helical and amphipathic structures as predicted by Edmundson projections (cf. Fig. 2A), or do they have some other structure? We have used CD and NMR spectroscopy to investigate the solution structure of citropin 1.1.

CD spectroscopy

CD spectra were acquired on citropin 1.1 in increasing concentrations (0–50%, v/v) of TFE in water. From 0 to 20% TFE, the CD spectra of citropin 1.1 showed a broad minimum at around 200 nm characteristic of an unstructured or random coil peptide. At concentrations of 30–50% TFE, the CD spectra exhibited two minima in the vicinity of 208 and 222 nm, indicating that citropin 1.1 adopts a predominantly α-helical structure under these solvent conditions. The greatest ellipticity at these minima occurred at 50% TFE suggesting maximal helical conformation at this concentration. Peptides with pronounced helical propensity reach a maximum helical content at concentrations such as this (i.e. 30–50% TFE) [47], suggesting citropin 1.1 has a high tendency to form a helical structure. Based on this evidence, NMR studies were performed using a 50% solution of the peptide in TFE/H_2O.

NMR spectroscopy

The ^{1}H NMR spectrum was assigned using XEASY software (v 1.3.13) [38] following the sequential assignment procedure [48], which involved the combined use of DQF-COSY, TOCSY and NOESY spectra. An HSQC spectrum was used to assign the α-^{13}C resonances from the one-bond correlations to the assigned ^{1}H resonances. Similarly, an HMBC spectrum was employed to make the carbonyl-^{13}C assignments from the two- and three-bond correlations to the assigned ^{1}H resonances. Table 3 lists all the assignments for the ^{1}H, α-^{13}C and carbonyl-^{13}C resonances.

The NH region of a NOESY spectrum in which a series of sequential NH to NH NOEs [$d_{NN}(i, i + 1)$] occur along the length of the peptide is shown in Fig. 3. A series of weaker

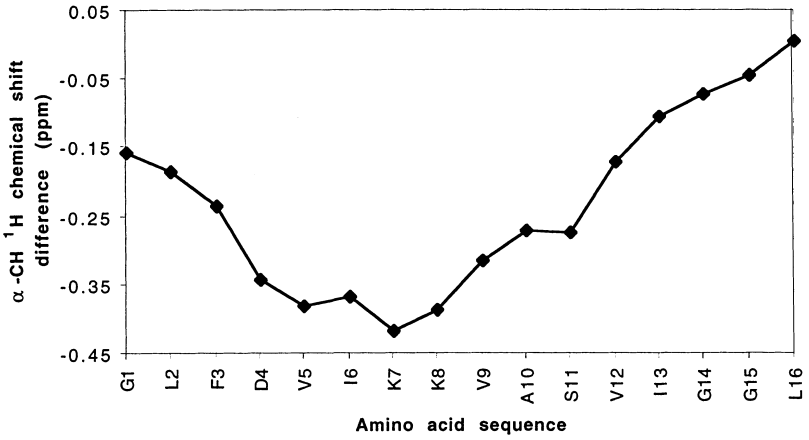

Fig. 5. Deviation from random-coil chemical shifts for the ^{1}H α-CH resonances of citropin 1.1 in 50% (v/v) d_3-TFE. A negative chemical shift difference indicates an upfield chemical shift compared to the random coil value [49]. The deviation values were smoothed over a window of $n = \pm 2$ residues [50].

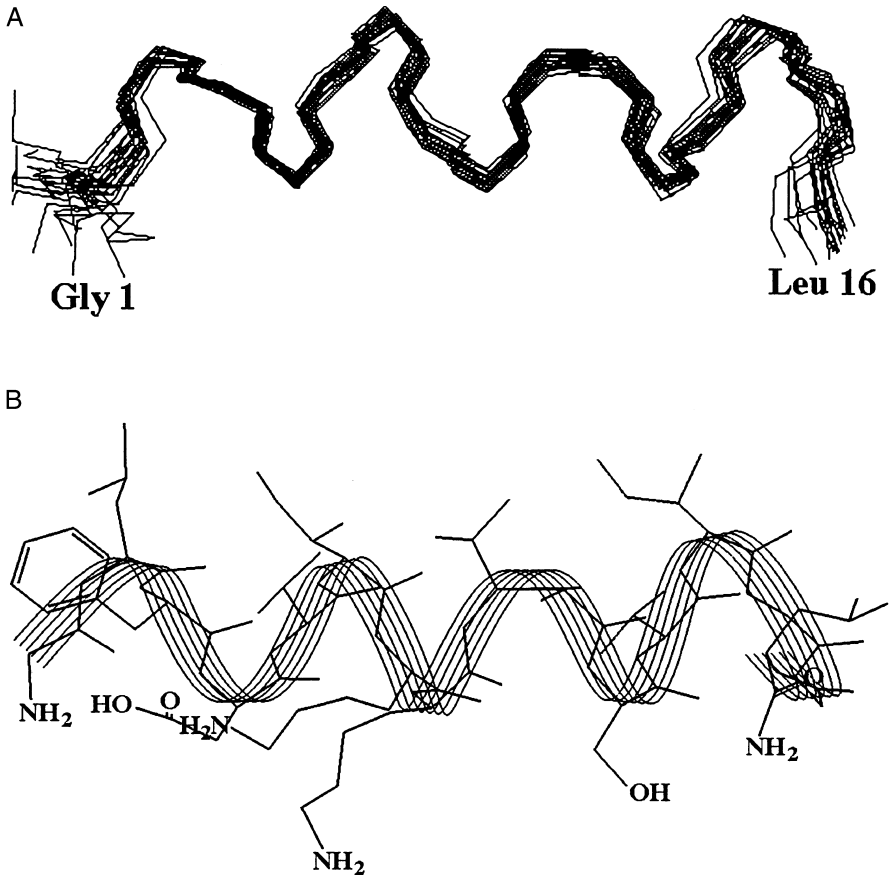

Fig. 6. (A) Superimposition of the 20 most stable structures of citropin 1.1, as viewed along their backbone atoms (N, α-C and carbonyl C) and (B) the most stable calculated structure of citropin 1.1. (B) A ribbon is drawn along the peptide backbone. The amphipathic nature of the peptide is apparent from this representation with the hydrophobic side above and the hydrophilic side below the polypeptide backbone.

$d_{NN}(i, i + 2)$ NOEs are also observed at a lower contour level in this region. A summary of the various types of NOEs observed for citropin 1.1 is presented in Fig. 4. Here it can be seen that in addition to the NOEs mentioned above, a number of weak sequential $d_{\alpha N}(i, i + 1)$ NOEs occur as well as a series of NOEs from residues three and four amino acids apart [$d_{\alpha N}(i, i + 3)$, $d_{\alpha\beta}(i, i + 3)$ and $d_{\alpha N}(i, i + 4)$]. Taken together, the observed NOEs and their intensities are consistent with citropin 1.1 having a helical structure along the majority of its sequence.

A helical structure for citropin 1.1 is also indicated from an examination of the deviation from random coil chemical shift values of the α-^{1}H, α-^{13}C and carbonyl-^{13}C resonances determined in water [48,49]. Smoothed over a window of $n = \pm 2$ residues [50], the plot for the ^{1}H α-CH resonances shows a distinct upfield shift (Fig. 5), while those for the ^{13}C resonances show a distinct downfield shift, except in the vicinity of the N- and C-termini. The directions of these deviations from random coil chemical shift values are consistent with the

Table 4. Structural statistics of citropin 1.1 following RMD/SA calculations. < SA > is the ensemble of the 20 final structures (SA) is the mean structure obtained by best-fitting and averaging the coordinates of backbone N, α-C and carbonyl-C atoms of the 20 final structures. $(SA)_r$ is the representative structure obtained after restrained energy minimization of the mean structure. Well-defined residues are those with angular order parameters (S) > 0.9. For citropin 1.1, residues Leu2 to Gly15 are well-defined.

RMSD from mean geometry (nm)	< SA >	$(SA)_r$
All heavy atoms	0.087 ± 0.016	–
All backbone atoms (N, α-C, carbonyl-C)	0.056 ± 0.016	–
Heavy atoms of well-defined residues	0.072 ± 0.013	–
Backbone atoms (N, α-C, carbonyl-C) of well-defined residues	0.037 ± 0.014	–
XPLOR energies (kcal·mol^{-1})		
E_{tot}	50.62 ± 2.37	46.19
E_{bond}	2.98 ± 0.18	2.66
E_{angle}	15.60 ± 1.01	13.85
$E_{improper}$	1.90 ± 0.42	1.27
E_{repel}	6.75 ± 1.03	5.09
E_{NOE}	23.39 ± 1.48	23.32
E_{cdih}	0.00 ± 0.01	0.00

peptide having a helical structure along its length, with maximal helicity in its central region and less well-defined structure at its N- and C-termini [51–53].

Structural analysis

The conclusions derived from an examination of the NMR data were confirmed when the NOE data were used as input for structural calculations. Sixty structures were generated by RMD and dynamical SA calculations and the 20 structures of lowest potential energy were selected for close examination. Some statistics for the 20 final structures are given in Table 4.

The superimposition of the 20 structures over the backbone N, α-C and carbonyl-C atoms shows that citropin 1.1 forms a regular α-helix along its entire length (Fig. 6a). Analysis of the angular order parameters (S, ϕ and ψ) [54] of these structures indicated that, except for the N- and C-terminal residues (Gly 1 and Leu 16), all residues were well defined with $S > 0.9$ for both their ϕ and ψ angles (not shown). The (ϕ,ψ) distribution (i.e. Ramachandran plot [55]) for the well-defined amino acids were all in the favoured region for α-helical conformation (not shown). The most energetically stable of the final 20 structures is displayed in Fig. 6b and from this representation it is apparent that citropin 1.1 forms an amphipathic α-helical structure with well-defined hydrophobic and hydrophilic faces.

Comparison of the observed NH chemical shifts of citropin 1.1 with the corresponding random coil NH chemical shifts [49] revealed a periodic distribution such that those from residues in the centre of the hybophobic face of the amphipathic face were shifted upfield with respect to the random coil values. This behaviour was first noted and investigated by Zhou *et al*. [56] in their CD and NMR study of a synthetic amphipathic helical peptide. They concluded that these variations in NH chemical shifts arise from a slight curvature of the amphipathic helix, which leads to differences in backbone hydrogen bond length along both faces of the peptide. In the case of citropin 1.1, it is apparent from Fig. 6b that the helix is slightly curved such that the hydrophobic face is concave, i.e. it has shorter hydrogen bonds than the hydrophilic side.

DISCUSSION

Citropins 1.1 and 1.2 are the major antibacterial and amphipathic peptides produced by both the dorsal and submental glands of *L. citropa.* These peptides are structurally dissimilar to the antimicrobial peptides of other tree-frogs of the genus *Litoria* that we have studied previously both in sequences and in length [46]. They are the simplest, amphibian, wide-spectrum antibacterial peptides reported to this time. They differ only in the nature of the hydrophobic residues at positions 5, 6, 12 and 13 in their sequence, and all contain the hydrophilic residues Asp4, Lys7 and 8 and Ser11. There is however, one feature of *L. citropa* that is similar to other tree-frogs of the genus *Litoria* that we have studied, i.e. they all produce endoproteases that deactivate the major antibacterial peptides after they have been on the skin for some period (after about 10 min for *L. citropa*: within the 5–30 minute range for other frogs we have studied [13,14]). In the case of caerin 1.1 and maculatin 1.1, endoproteases remove the first two amino acid residues effectively deactivating each peptide [13,14], while citropins 1.1 and 1.2 are principally degraded by the removal of three residues, with peptides with two missing residues being formed in much smaller yield (see Tables 1 and 2 for sequence and activity data, respectively) (cf. also the degradation of the magainin peptides from *X. laevis* [57]). The citropin peptides show little sequence similarity to other antibacterial peptides from frogs of the genus *Litoria* so far studied, but they do show an overall structural resemblance to the 17 residue uperin 3 antibacterial peptides that are produced by toadlets of the genus *Uperoleia* [58]. For example, compare the sequences of uperin 3.6 (a major antibacterial peptide of *Uperoleia mjobergii*) and citropin 1.1.

Uperin 3.6 GVI**D**AA**KK**VVNVLKNLF-NH_2

Citropin 1.1 GLF**D**VI**KK**VASVIGGL-NH_2

These two peptides have a very similar distribution of hydrophobic and hydrophilic amino acids, in particular the three conserved charged amino acids which are highlighted in bold. In addition to these amino acids, uperin 3.6 contains an additional Lys at residue 14. The spectrum of antibacterial activity of uperin 3.6 is very similar to those of citropin 1.1, 1.2 and 1.3 (see Table 2). The solution structure of uperin 3.6 has been investigated by NMR techniques [59], and like citropin 1.1, it is a well defined amphipathic α-helix along the entire length.

Although citropin 1.1 is almost entirely helical in the membrane-mimicking solvent TFE (Fig. 6), the length (16 amino acids) is too short to span the lipid bilayer. The potent antibacterial activity of citropin 1.1 cannot therefore arise from simple aggregation of the peptides in an orientation perpendicular to the bilayer plane to form a pore (e.g. via the barrel-stave mechanism). Other mechanisms for the lytic activity of the antibacterial citropin and uperin peptides must therefore be invoked, e.g. those involving the orientation of the peptides parallel to the membrane surface where they either aggregate in a carpet like manner [19] or diffuse continuously throughout the membrane [21]. In both instances, destabilization of the membrane occurs which creates openings within the bilayer.

What are the roles of the citropin 2 and 3 peptides in the amphibian integument? The complex citropin 2 and 3 peptides (Table 1) have not shown significant antibacterial activity in our testing regime. The role of the basic citropin 2 peptides is not known at this time. The citropin 3 peptides are quite unusual in that (a) the sequence commences with Asp (the only other reported amphibian peptides that commence with Asp are hylambin [1] and kassinin [1]; both members of the tachykinin family of neuropeptides which bear no structural relationship to the citropins 2 and (b) they are anionic peptides. The anionic nature of the peptides suggests that they may be spacer peptides for the procitropin 1 peptides within the dorsal and submental glands (see [60] for a review of the biosynthesis of antibiotic peptides), although this proposal has not been confirmed.

Finally, the role of the four extra citropin 1 peptides from the dorsal gland secretion (I to L in Fig. 2 and Table 1), is, to date, a mystery. The four extra citropin 1 peptides are related structurally, two to citropin 1.1 and two to citropin 1.2. The last two residues of the citropins 1.1 and 1.2 have been replaced by Leu-Asp and two extra residues (either Ser-Pro-OH or Ser-Gln-OH) added. One of these peptides, citropin 1.1.3, has been tested for antibacterial activity, but such activity is insignificant (see Table 2). Perhaps these peptides are hormones or neuropeptides. If so, they bear no structural resemblance to any known amphibian hormone or neuropeptide: they are certainly not related to the potent amphibian caerulein or uperolein type neuropeptide vasodilators [1,2,45,46].

ACKNOWLEDGEMENTS

This work was financed by the Australian Research Council. K.L.W., P.A.W. and B.C.S.C. acknowledge the awards of an Australian Postgraduate Award, an ARC PhD scholarship, and an Overseas Australian

Postgraduate Award, respectively. We thank Mr G. Beardsell for providing access to a specimen of *L. citropa*, Ms D. Turner for automated peptide sequencing, and Dr R. Lindner for assistance with acquisition and processing of the CD spectra.

REFERENCES

1. Lazarus, L.H. & Attila, M. (1993) The toad, ugly and venomous, wears yet a precious jewel in his skin. *Prog. Neurobiol.* **41**, 473–507.
2. Erspamer, V. (1994) Bioactive secretions of the amphibian integument. In *Amphibian Biology. The Integument* (Heatwold, H., ed.), Vol. 1, pp. 178–350, Surrey Beatty, Chipping Norton, Australia.
3. Bevins, C.L. & Zasloff, M. (1990) Peptides from frog skin. *Annu. Rev. Biochem.* **59**, 395–414.
4. Barra, D. & Simmaco, M. (1995) Amphibian skin: a promising resource for antimicrobial peptides. *Trends Biotech.* **13**, 205–209.
5. Soballe, P.W., Maloy, W.L., Myrga, M.L., Jacob, L.S. & Herlyn, M. (1995) Experimental local therapy of human melanoma with lytic magainin peptides. *Int. J. Cancer* **60**, 280–284.
6. Jacob, L. & Zasloff, M. (1994) Potential therapeutic applications of magainins and other antimicrobial agents of animal origin. *Ciba Found. Symposium* **186**, 197–223.
7. Stone, D.J.M., Bowie, J.H., Tyler, M.J. & Wallace, J.C. (1992) The structure of caerin 1.1, a novel peptide from Australian tree frogs. *J. Chem. Soc. Chem. Commun.* 1224–1225.
8. Stone, D.J.M., Waugh, R.J., Bowie, J.H., Wallace, J.C. & Tyler, M.J. (1992) Peptides from Australian frogs. Structures of the caerins and caeridins from *Litoria splendida*. *J. Chem. Soc. Perkin Trans.* **1**, 3173–3178.
9. Stone, D.J.M., Waugh, R.J., Bowie, J.H., Wallace, J.C. & Tyler, M.J. (1993) Peptides from Australian frogs. The structures of the caerins from *Litoria caerulea*. *J. Chem. Res.* **S**, 138; **M**, 910–936.
10. Waugh, R.J., Stone, D.J.M., Bowie, J.H., Wallace, J.C. & Tyler, M.J. (1993) Peptides from Australian frogs. The structures of the caerins and caeridins from *Litoria gilleni*. *J. Chem. Res.* **S**, 139; **M**, 937–961.
11. Waugh, R.J., Steinborner, S.T., Bowie, J.H., Wallace, J.C., Tyler, M.J., Hu. P. & Gross, M.L. (1995) Two isomeric α and β aspartyl dodecapeptides and their cyclic amino-succinyl analogue from the Australian green tree frog *Litoria gilleni*. *Aust. J. Chem.* **48**, 1981–1987.
12. Steinborner, S.T., Waugh, R.J., Bowie, J.H., Tyler, M.J. & Wallace, J.C. (1997) New caerin antibacterial peptides from the skin glands of the tree frog *Litoria xanthomer*. *J. Peptide Sci.* **3**, 181–185.
13. Steinborner, S.T., Currie, G.J., Bowie, J.H., Wallace, J.C. & Tyler, M.J. (1998) New caerin 1 peptides from the skin glands of the Australian tree frog *Litoria chloris*. A comparison of the antibiotic activities of the caerin 1 peptides. *J. Peptide Res.* **51**, 121–126.
14. Rozek, T., Waugh, R.J., Steinborner, S.T., Bowie, J.H., Wallace, J.C. & Tyler, M.J. (1998) The maculatin peptides from the skin glands of the tree frog *Litoria genimaculata*. A comparison of the antibacterial activities of maculatin 1.1 and caerin 1.1. *J. Peptide Sci.* **4**, 111–115.
15. Wong, H., Bowie, J.H. & Carver, J.A. (1997) The solution structure and activity of caerin 1.1, an antimicrobial peptide from the Australian tree frog, *Litoria splendida*. *Eur. J. Biochem.* **247**, 545–557.
16. Chia, B.C.S., Carver, J.A. & Bowie, J.H. (1999) Maculatin 1.1, an antimicrobial peptide from the Australian tree frog, *Litoria genimaculata*: solution structure and activity studies. *Protein Sci.* (submitted).
17. Arseniev, A.S., Barsukov, V.F., Bystro, V., Lomize, A.L. & Ovchinnikov, Y.A. (1985) ^{1}H-NMR study of gramicidin A transmembrane ion channel: head-to-head right-handed, single-stranded helices. *FEBS Lett.* **186**, 168–174.
18. Marion, D., Zasloff, M. & Bax, A. (1988) A two-dimensional NMR study of the antimicrobial peptide magainin 2. *FEBS Lett.* **227**, 21–26.
19. Shai, Y. (1995) Molecular recognition between membrane-spanning peptides. *Trends Biochem. Sci.* **20**, 460–464.
20. Eland, R.M., Shai, Y.C., Segrest, J.P. & Anantharamaiah, G.M. (1995) Mechanisms for the modulation of membrane bilayer properties by amphipathic helical peptides. *Biopolymers* **37**, 319–338.
21. Bechinger, B. (1997) Structure and function of channel forming peptides, magainins, cecropins, melittin and alamethicin. *J. Mem. Biol.* **156**, 197–211.
22. Matsuzaki. K. (1998) Magainins as paradigm for the mode of action of pore forming polypeptides. *Biochim. Biophys. Acta* **1376**, 391–400.
23. Bechinger, B., Zasloff, M. & Opella, S.J. (1993) Structure and orientation of the antibiotic peptide magainin in membranes by solid-state NMR. *Protein Sci.* **2**, 2077–2084.
24. Dumeril, A.M.C. & Bibron, G. (1841) *Erpétologie Générale Ou Histoire Naturelle Complète Des Reptiles*, Vol. 9. Libraire Roret, Paris.
25. Barker, J., Grigg, G.C. & Tyler, M.J. (1995) In *A Field Guide to Australian Frogs*, pp. 40–53. Surrey, Beatty and Sons, Chipping Norton, Australia.
26. Tyler, M.J., Stone, D.J.M. & Bowie, J.H. (1992) A novel method for the release and collection of dermal glandular secretions from the skin of frogs. *J. Pharmacol. Toxicol. Methods* **28**, 199–200.
27. Hunkapiller, M.W., Hewick, R.M., Drewer, W.J. & Hood, L.E. (1983) *Methods Enzymol.* **91**, 399–406.
28. Maeji, N.J., Bray, R.M., Valerio, R.M. & Wang, W. (1995) Larger scale multipin peptide synthesis. *Peptide Res.* **8**, 33–38.
29. Jorgensen, J.H., Cleeland, W.A., Craig, G., Doern, M., Ferraro, J., Finegold, C.M., Hansen, S.L., Jenkins, S.G., Novick, W.J., Pfaller, M.A., Preston, D.A., Reller, L.B. & Swenson, J.M. (1993) Methods for dilution antimicrobial susceptibility tests for bacteria that grow aerobically, 3rd approved standard. In *National Committee for Clinical Laboratory Standards (Document M7–A3)*, Vol. 13, pp. 1–12.
30. Rance, M., Sørrenson, O.W., Bodenhausen, G., Wagner, G., Ernst, R.R. & Wüthrich, K. (1983) Improved spectral resolution in COSY ^{1}H-NMR spectra of proteins via double quantum filtering. *Biochem. Biophys. Res. Commun.* **117**, 479–485.
31. Davis, D.G. & Bax, A. (1985) Assignment of complex ^{1}H NMR spectra via two-dimensional homonuclear Hartmann-Hahn spectroscopy. *J. Am. Chem. Soc.* **107**, 2820–2821.
32. Jeener, J., Meier, B.H., Bachman, P. & Ernst, R.R. (1979) Investigation of exchange processes by two-dimensional NMR spectroscopy. *J. Chem. Phys.* **71**, 4546–4553.
33. Marion, D. & Wüthrich, K. (1983) Application of phase sensitive two-dimensional correlated spectroscopy (COSY) for measurements of ^{1}H-^{1}H spin-spin coupling constants in proteins. *Biochem. Biophys. Res. Commun.* **113**, 967–974.
34. John, B.K., Plant, D., Webb, P. & Hurd, R.E. (1992) Effective combination of gradients and crafted RF pulses for water suppression in biological samples. *J. Magn. Reson.* **98**, 200–206.
35. Griesinger, C., Otting, G., Wüthrich, K. & Ernst, R.R. (1988) Clean TOCSY for ^{1}H spin system identification in macromolecules. *J. Am. Chem. Soc.* **110**, 7870–7872.
36. Kay, L.E., Keifer, P. & Saaringen, T. (1992) Pure absorption gradient enhanced heteronuclear single quantum correlation spectroscopy with improved sensitivity. *J. Am. Chem. Soc.* **114**, 10663–10665.
37. Summers, M.F., Marzilli, L.G. & Bax, A. (1986) Complete ^{1}H and ^{13}C assignments of coenzyme B_{12} through the use of new two-dimensional NMR experiments. *J. Am. Chem. Soc.* **108**, 4285–4294.
38. Bartels, C., Xia, T.H., Billeter, M., Güntert, P. & Wüthrich, K. (1995) The program XEASY for computer supported NMR spectral analysis of biological macromolecules. *J. Biomol. NMR* **6**, 1–10.
39. Xu, R.X., Word, J.M., Davis, D.G., Rink, M.J., Willard, D.H. & Gampe, R.T. (1995) Solution structure of the human pp60c-src SH2 domain complexed with a phosphorylated tyrosine pentapeptide. *Biochemistry* **34**, 2107–2121.
40. Brunger, A.T. (1992) *A System for X-ray Crystallography and NMR, in X-PLOR (Version 3.851)*. Yale University, New Haven, CT.
41. Brunger, A.T. & Nilges, M. (1993) Computational challenges for macromolecular structure determination by X-ray crystallography and solution NMR-spectroscopy. *Q. Rev. Biophys.* **26**, 49–125.
42. Nilges, M., Kuszewski, J. & Brunger, A.T. (1992) Sampling properties

of simulated annealing. In *Proceedings of the NATO Advanced Research Workshop on Computational Aspects of the Study of Biological Macromolecules by NMR*. Il Ciocco, Italy.
43. Folmer, R.H.A., Hilbers, C.W., Konings, R.N.H. & Nilges, M. (1997) Floating stereospecific assignment revisited – application to an 18 kDa protein and comparison with J-coupling data. *J. Biomol. NMR* **9**, 245–258.
44. Engh, R.A. & Huber, R. (1991) Accurate bond and angle parameters for x-ray protein structure refinement. *Acta Crystallogr.* **A47**, 392–400.
45. Bowie, J.H., Chia, B.C.S. & Tyler, M.J. (1998) Host defence peptides from the skin glands of Australian amphibians: a powerful chemical arsenal. *Pharm. News.* **5**, 16–21.
46. Bowie, J.H., Wegener, K.L., Chia, B.C.S., Wabnitz, P.A., Carver, J.A., Tyler, M.J. & Wallace, J.C. (1999) Host defence antibacterial peptides from skin secretions of Australian amphibians. The relationship between structure and activity. *Prot. Pept. Lett.* (in press).
47. Sönnichsen, F.D., Van Eyk, J.E., Hodges, R.S. & Sykes, B.D. (1992) Effect of trifluoroethanol on protein secondary structure: an NMR and CD study using a synthetic actin peptide. *Biochemistry* **31**, 8790–8798.
48. Wüthrich, K. (1986) *NMR of Proteins and Nucleic Acids*. Wiley, New York.
49. Wishart, D.S., Bigam, C.G., Holm, A., Hodges, R.S. & Sykes, B.D. (1995) ^{1}H, ^{13}C and ^{15}N random coil NMR chemical shifts of the common amino acids. I. Investigations of nearest-neighbour effects. *J. Biomol. NMR* **5**, 67–81.
50. Pastore, A. & Saudek, V. (1990) The relationship between chemical shift and secondary structure. *J. Magn. Reson.* **90**, 165–176.
51. Wishart, D.S., Richards, F.M. & Sykes, B.D. (1991) Relationship between NMR chemical shift and protein secondary structure. *J. Mol. Biol.* **222**, 311–333.
52. Wishart, D.S., Richards, F.M. & Sykes, B.D. (1992) The chemical shift index: a fast and simple method for the assignment of protein secondary structure through NMR spectroscopy. *Biochemistry* **31**, 1647–1651.
53. Wishart, D.S. & Sykes, B.D. (1994) The ^{13}C chemical-shift index: a simple method for the identification of protein secondary structure using ^{13}C chemical-shift data. *J. Biomol. NMR* **4**, 171–180.
54. Pallaghy, P.K., Duggan, B.M., Pennington, M.W. & Norton, R.S. (1993) 3-Dimensional structure in solution of the calcium channel blocker ω-conotoxin. *J. Mol. Biol.* **234**, 405–420.
55. Morris, A.L., MacArthur, M.W., Hutchinson, E.G. & Thornton, J.M. (1992) Stereochemical quality of protein structure coordinates. *Proteins* **12**, 345–364.
56. Zhou, N.E., Zhu, B.-Y., Sykes, B.D. & Hodges, R.S. (1992) Relationship between amide proton chemical shifts and hydrogen bonding in amphipathis α-helical peptides. *J. Am. Chem. Soc.* **114**, 4320–4326.
57. Resnick, N., Maloy, W., Crut, H. & Zasloff, M. (1991) A novel endopeptidase from *Xenopus* that recognises α-helical structure. *Cell* **66**, 541–554.
58. Bradford, A.M., Bowie, J.H., Tyler, M.J. & Wallace, J.C. (1996) New antibiotic peptides from the dorsal glands of the Australian toadlet *Uperoleia mjobergii. Aust. J. Chem.* **49**, 1325–1331.
59. Chia, B.C.S., Mulhern, T.D., Carver, J.A. & Bowie, J.H. (1999) The solution structure of uperin 3.6, an antibiotic peptide from the granular dorsal glands of the Australian toadlet, *Uperoleia mjobergii. J. Peptide. Res.* **54**, 137–145.
60. Ganz, T. (1994) Biosynthesis of defensins and other antimicrobial peptides. In *Ciba Symposium* (Boman, H.G., Marsh, J. & Goode, J.A., eds), Vol. 186, pp. 62–76. Wiley, Chichester.

SUPPLEMENTARY MATERIAL

The following material is available from http://www.blackwell-science.com/ejb/

Fig. S1. CD spectra of citropin 1.1 at the varying concentrations (v/v) of trifluoroethanol (TFE) indicated.

Fig. S2. Deviation from random coil chemical shifts [49] of (a) α-^{13}C and (b) carbonyl ^{13}C resonances of citropin 1.1 in 50% (v/v) d_3-TFE. A positive chemical shift difference indicates a downfield chemical shift compared to the random coil value. The deviation values were smoothed over a window of $n = \pm 2$ residues [50].